



## CASE STUDY OF WIND-RESISTANT DESIGN AND ANALYSIS OF HIGH MAST STRUCTURES BASED ON DIFFERENT WIND CODES

Ching-Wen Chien

*Department of Harbor and River Engineering, National Taiwan Ocean University, Keelung, Taiwan, R.O.C. Project Group-Power Projects, E&C Engineering Corporation, d93520010@mail.ntou.edu.tw*

Jing-Jong Jang

*Department of Harbor and River Engineering, National Taiwan Ocean University, Keelung, Taiwan, R.O.C.*

Follow this and additional works at: <https://jmstt.ntou.edu.tw/journal>



Part of the [Civil and Environmental Engineering Commons](#)

### Recommended Citation

Chien, Ching-Wen and Jang, Jing-Jong (2008) "CASE STUDY OF WIND-RESISTANT DESIGN AND ANALYSIS OF HIGH MAST STRUCTURES BASED ON DIFFERENT WIND CODES," *Journal of Marine Science and Technology*: Vol. 16: Iss. 4, Article 6.

DOI: 10.51400/2709-6998.2013

Available at: <https://jmstt.ntou.edu.tw/journal/vol16/iss4/6>

This Research Article is brought to you for free and open access by Journal of Marine Science and Technology. It has been accepted for inclusion in Journal of Marine Science and Technology by an authorized editor of Journal of Marine Science and Technology.

# CASE STUDY OF WIND-RESISTANT DESIGN AND ANALYSIS OF HIGH MAST STRUCTURES BASED ON DIFFERENT WIND CODES

Ching-Wen Chien\* and Jing-Jong Jang\*\*

Key words: high mast structure (HMS), wind-resistant design (WRD), gust effect factor (GEF).

## ABSTRACT

The high mast structure (HMS) has the characters of light weight and high cost efficiency. Therefore, it is widely used in the modern construction industry. It has a large the ratio of height (H) to least horizontal dimension (D) that makes it a particularly more slender and wind-sensitive than any other structures. Therefore, the purpose of this research is to develop the wind-resistant design (WRD) procedure for the slender, tapered support structures of HMS subjected to wind-induced excitation from vortex shedding and gust buffeting. This paper illustrates the theoretical basis and the analytical development of the WRD; including calculating gust effect factor (GEF) in along-wind respond; lock-in and galloping effects in across-wind respond. The finite element program is used to analyze the natural period and displacement of HMS in this study. The results of this research highlight the following three parts. First, it is a good verification that natural periods of one second can be used in the discrimination of to rigidity and flexible structure in gust effect factor (GEF) analysis procedure for HMS. Second, the across-wind displacement of HMS should be considered in analysis for WRD procedure. Third, the wind-induced vibration and instability behaviors can be avoided by controlling the critical wind velocity in WRD procedure.

## I. INTRODUCTION

Up to today, the design of high mast structure (HMS) is applied to a large number of structures around the world to represent a relevant economic problem. The use of old codes,

developed by considering other kinds of structures, is unjustified in this sector. Taiwan's code [26] on wind actions and effects on structures as well as other standards of the new generation [4, 6] cannot be applied to these constructions. Some failures of poles and monotubular tower repeatedly confirmed the necessity of understanding better their wind-excited behaviour [24]. Facing these situations, developing of wind-resistant design (WRD) procedure for HMS is inspired by A.G. Davenport's the wind-load chain [11, 13, 14] and based on AASHTO, "Supports Specifications" [1, 2]. The geometry properties and wind effects on the existing HMS in Taiwan are investigated for WRD procedure.

On the other hand, vortex shedding is almost always present with bluff-shaped cylindrical bodies. In wind tunnel testing, it was found that large diameter round monotube mast arms would exhibit vortex shedding when there was no sign panel [16]. However, when the tip was installed the sign panel, galloping was occurred rather than the vortex shedding. The pioneering work of Scruton in the 1950s established some criteria in relation to a mass-damping parameter to check the aerodynamic in across-wind [20].

As for HMS significant problems can occur in more than one mode, particularly in the first four modes [28]. The contributions of high natural frequency components are investigated by eigenvalue analysis. Furthermore, how to check vortex resonance area and galloping calculation procedure in higher modes is also presented. The WRD procedure is proposed to suit for HMS, by means of controlling the wind-excited; mechanical response; design criteria, even clarifying with comparison of codes. Two cases of HMS in Taiwan [7, 8, 27] are studied to illustrate different physical phenomena and mechanical behaviors subjected to wind-induced effects in the actual local condition. It can be divided into four important parts to discuss in WRD procedure of HMS: (1) geometric properties and shape factors; (2) mean wind speed; (3) gust effect factor and (4) across-wind response.

## II. STRUCTURE PROPERTIES OF HMS

### 1. Geometric Properties

Typically, there are usually some functional equipments on the top of the structure such as a wind-force turbine, a radio

Paper submitted 05/31/07; accepted 11/03/07. Author for correspondence: Ching-Wen Chien (e-mail: d93520010@mail.ntou.edu.tw).

\*Department of Harbor and River Engineering, National Taiwan Ocean University, Keelung, Taiwan, R.O.C.

\*\*Project Group-Power Projects, E&C Engineering Corporation

\*\*Department of Harbor and River Engineering, National Taiwan Ocean University, Keelung, Taiwan, R.O.C.

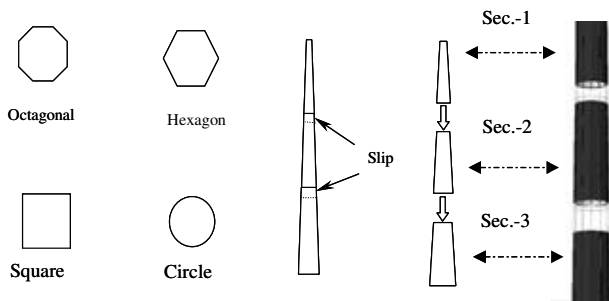


Fig. 1. Shapes and slip of the taper HMS.

wave transmitter, a radar, lamps and lanterns. The combination of the slender structural and the concentrated mass at the tip makes the structure fully aeroelastic and unstable. Generally, HMS is designed a taper; slender; multi-sides for lighting and telecommunication purposes. To meet these specific mounting height requirements the shaft may consist of more than one section to be assembled on site by means of the "slip on joint" as shown in Fig. 1. In the past several years, many accidents and much damage were caused by high wind or wind-induced vibrations in such structures.

They are never excessively high, for instance, high mast lighting structure (HMLS) always design in the range of 30 to 40 (m) height. Fig. 2 shows the ratio of diameter-thickness (D/t) to height for HMLS in Taiwan. Generally, when the D/t ratio of HMS is larger than 125, WRD is must considered to check the local buckling of the shaft. Traditionally, when the structure is tapered, designer usually adopts the average of diameter or uses the diameter at  $z=2/3h$  (the slope should be less than 2%) to analyze [28]. The recommended value of damping is 0.3~2.9% for steels masts and towers [22], it is assumed to be 2% in this study [18].

2. Shape Factors

There is a regular progression of drag coefficient ( $C_d$ ), while uplift coefficient ( $C_{0l}$ ) is extremely variable;  $C'_d$ ,  $C'_{0l}$  are the prime angular derivatives of  $C_d$ ,  $C_{0l}$ . In the limit case of circular section  $C_d$  is constant and  $C_{0l}=0$ ; then  $C'_d = C'_{0l} = 0$  [24].

For HMS with a polygon shape in plan, it may be assumed to all cases that windward coefficient ( $C_w$ )=0, so that the total drag coefficients:  $C_d=C_w+C_l=C_b$ ,  $C_w$ ,  $C_l$  are the values, averaged over the width of shaft, of the mean pressure coefficient on the windward face and suction coefficients on the leeward face, respectively. Increasing the number of sides of the polygon  $C_d$  is more and more regular while  $C_w$  and  $C_{0l}$  tends to be zero. For engineering purposes,  $C_{0l}=C'_d=0$  independently of the shape of the polygon;  $C'_{0l}=0$  is acceptable only for regular polygons with more than eight sides [10].

The recommended value of shape factor (drag coefficients of the shaft) is 0.6~0.8 for a 16-polygons or circular section of HMS. In this study, it is assumed to be 0.6 for shaft [26]; a drag coefficient of 1.0 was assumed for luminaries or blades of structure at the top [2, 16].

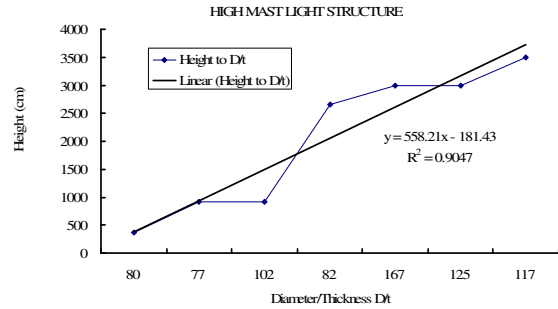


Fig. 2. Height vs. D/t of the HML support structure.

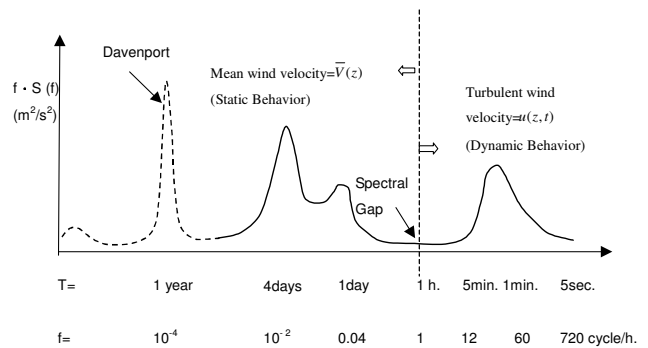


Fig. 3. Autospectra for the wind velocity (After Van der Hovorn 1957).

III. WIND-INDUCED RESPONSE

1. Characters of Wind Velocity

Fig. 3 shows the Van der Hovorn spectrum, which is based on measurements at about 100m height near Brookhaven New York of U.S.A. The ordinate is the frequency  $f$  multiplied by the autospectrum  $S(f)$  for the horizontal wind velocity. The spectral gap of nearly 1hr means that the wind climate for left side and the turbulence in the atmospheric boundary layer for right side is mutually independent as Fig. 3, so it may be treated separately and superimposed.

The gust wind velocity  $\bar{V}(z) + u(z,t)$  is separated into a wind climate component  $\bar{V}(z)$  and a turbulence component  $u(z,t)$ . The wind climate component  $\bar{V}(z)$  is measured per 10 minutes by mean wind velocity and the turbulence component  $u(z,t)$  is here calculated with an average time of 10s.

2. Mean of Wind Velocity

The relation  $\bar{V}_t(z)$  of  $t$  second to  $\bar{V}_{3600}(z)$  of 1 hour given by

$$\bar{V}_t(z) = \bar{V}_{3600}(z) + c(t) \cdot [u^2]^{1/2} \tag{1}$$

where  $c(t)$  is a coefficient;  $u$  is longitudinal turbulent fluctuation

**Table 1. Coefficients of  $c(t)$ .**

Sec.	1	10	20	30	50	100	200	300	600	1000	3600
$c(t)$	3.00	2.32	2.00	1.73	1.35	1.02	0.07	0.54	0.36	0.16	0.00

$$\overline{u^2} = \beta \cdot u_*^2 \tag{2}$$

where  $u_*$  is the shear velocity, via Logarithmic Law, then is given by

$$\overline{V}_{3600}(z) = \frac{1}{k} u_* \ln\left(\frac{z - z_d}{z_0}\right) \Rightarrow u_* = \frac{k \cdot \overline{V}_{3600}(z)}{\ln\left(\frac{z - z_d}{z_0}\right)} \tag{3}$$

Substituting Eq. (2) into Eq. (1), then become

$$\overline{V}_i(z) = \overline{V}_{3600}(z) + c(t) \cdot [\beta \cdot u_*^2]^{1/2} \tag{4}$$

$Z_0$  is the roughness length, which is a constant for a surface of given roughness. It follows that Eqs. (3) and (4) become

$$\overline{V}_i(Z) = \overline{V}_{3600}(Z) + c(t) \cdot \beta^{1/2} \cdot \overline{V}_{3600}(Z) \cdot \frac{k}{\ln\left(\frac{z}{z_0}\right)} \tag{5}$$

Assuming  $Z_d = 0, \beta = 6.0$  (Solari 1982 [23]),  $k = 0.4$  (Karman Constant) substituted into Eq. (5) to obtain the Eq. (6),  $c(t)$  is shown as in Table 1.

$$\overline{V}_i(Z) = \overline{V}_{3600} \cdot \left[ 1 + \frac{\sqrt{\beta} c(t) k}{\ln(z/z_0)} \right] = \overline{V}_{3600}(Z) \cdot \left[ 1 + \frac{0.98 c(t)}{\ln\left(\frac{z}{z_0}\right)} \right] \tag{6}$$

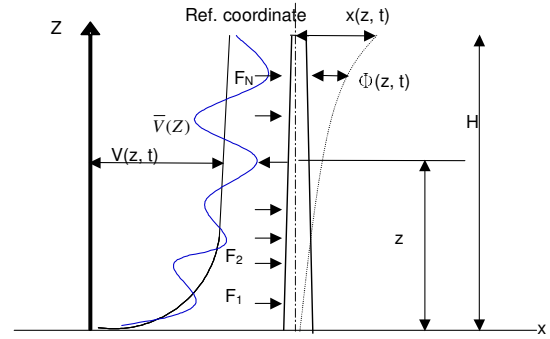
### 3. Along-Wind Force

Fig. 4 depicts a turbulent wind profile impinging on a HMS. The mean intensity of wind loading at any point will be given by

$$\overline{P}(z) = \frac{1}{2} \cdot \rho \cdot \overline{V}^2(z) \cdot C_d \cdot B(z) \tag{7}$$

where  $B(z)$  is the width of structure transverse to the wind with height is changed.  $C_d$  is the total drag coefficient ( $=C_w + C_l$ ).  $\rho$  is the density of air  $\approx 1.2\text{kg/m}^3$ ,  $\overline{V}(z)$  is the mean wind speed at height  $z$ . Typically, the generalized coordinate is selected as the displacement of some convenient reference point in the system, such as the tip displacement in this HMS. Assuming that  $\phi(z) = \left(\frac{z}{H}\right)^\xi$ ,  $\xi$  is the mode exponent and by integrating the mean intensity of wind loading over the height of HMS the familiar express gives at any point will be given by

$$F_d = \overline{E} = \frac{1}{2} \cdot C_d \cdot B(z) \cdot \int_0^H \overline{V}(z)^2 \cdot \phi(z) dz \tag{8}$$



**Fig. 4. Behaviors of the mast structure subjected to wind loading.**

Then, the mean displacement of mean along-wind velocity at the average of  $z$  height is obtained by Eq. (9).

$$\overline{X}_{ave} = \frac{F_d}{K_1}; K_1 = m_1 (2\pi n_1)^2 \tag{9}$$

where  $K_j$  is the generalized stiffness of the structure;  $m_1$  and  $n_1$  are the first mode of generalized mass and natural frequency, respectively. The wind vector at any point may be regarded as the sum of the mean wind vector and a dynamic component, is given by  $V(z,t) = \overline{V}(z) + u(z,t)$ . The distributed loading is  $F(z) = \overline{P}(z) + p(z,t)$  due to wind at height  $z$ ; where  $\overline{P}(z)$  and  $p(z,t)$  are the mean and fluctuating components, respectively. In terms of velocities, Eq. (7) becomes

$$F(z) = \frac{1}{2} \rho [\overline{V}(z) + u(z,t)]^2 \cdot C_d \cdot B(z) \tag{10}$$

Since the second-order term in  $u^2(z,t)$  can be ignored in comparison with  $\overline{V}^2(z)$ . Hence, the fluctuating component will be given by

$$p(z,t) = \rho \cdot \overline{V}(z) \cdot u(z,t) \cdot C_d \cdot B(z) \tag{11}$$

However, the load effect on an element of the structure will be

$$dE(t) = \rho \cdot \overline{V}(z) \cdot u(z,t) \cdot C_d \cdot B(z) \cdot dz \tag{12}$$

Furthermore, the effect of the randomly distributed fluctuating forces on the dynamic response of the structure will be explained with ref. Fig. 4. If the forces are considered as discrete forces, then the total load on the structure will be

$$F = F_1 + F_2 + \dots + F_i + \dots + F_N = \sum_i^N F_i \tag{13}$$

$$F_i(z,t) = \overline{P}(z) + p(z,t) \tag{14}$$

The square of the total load will therefore be

$$F^2 = F_1^2 + F_2^2 + \dots + F_i F_j + \dots + F_N^2 = \sum_i^N \sum_j^N F_i F_j \tag{15}$$

The mean square load will hence be obtained by averaging Eq. (15) over an appropriate period, e.g. one hour. Replacing  $F_i$  and  $F_j$  by distributed loading at any two points ( $z, z'$ ), and per-

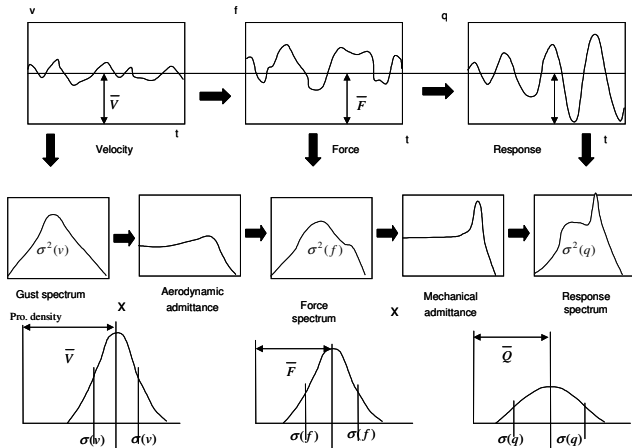


Fig. 5. Normal spectra method (after Davenport).

forming a double integral over the height of the structure one can find the mean square load effect is

$$\begin{aligned}\sigma_B^2(E) &= \rho^2 C_d^2 B^2 \int_0^H \int_0^H \overline{(\bar{V}(z)u(z,t)) \cdot (\bar{V}(z)u(z,t))} dz dz' \\ &= \rho^2 C_d^2 B^2 \int_0^H \int_0^H \sigma_x \sigma_x' \bar{V}(z) \bar{V}(z') R(z, z') dz dz'\end{aligned}\quad (16)$$

The cross-correlation coefficient is given by

$$R(z, z') = \overline{u(z, t) \cdot u(z', t)} / \sigma_x \cdot \sigma_x' \quad (17)$$

It is reasonable to ignore the variation of  $\sigma_x^2$  with height, using  $\sigma_x = 2.5v_s$  [22]. Therefore, the expression becomes

$$\sigma_B^2(E) = \rho^2 C_d^2 B^2 \sigma_x^2 \int_0^H \int_0^H \bar{V}(z) \bar{V}(z') R(\Delta z) dz dz' \quad (18)$$

where  $R(\Delta z) = e^{-\Delta r/L}$ ;  $\Delta r = z - z'$ ;  $L$  is lateral scale ( $\doteq 60m$ ) [22]. The double integration has to be performed numerically in general. However, by recasting Eq. (18) in a non-dimensional form it has been possible to derive charts from which the response of a wide range of structures may be evaluated with ease.

#### 4. Gust Effect Factor (GEF) Methods

The gust component is considered as a random process and may thus be described by a gust spectrum with variance  $\sigma^2(v)$  as shown in Fig. 5. A practical procedure was suggested by Davenport. He was able to derive a factor which the *R.M.S.* (Root Mean Square) component would be exceeded with a probability of 50%. After further refinement Davenport recommended the following expression for peak factor

$$g = \sqrt{2 \times \ln(vT_0)} + \frac{\gamma}{\sqrt{2 \times \ln(vT_0)}} \quad (19)$$

$\gamma = 0.577$  is Euler's constant;  $T_0$  is the period during which the peak response is assumed to occur. Thus, maximum instantaneous wind velocity is then  $V_{MAX} = V + g \cdot \sigma(V)$ . Usually,  $T_0$  is the 1hr.=3600 second;  $V$  is the expected frequency; clearly equal to the natural frequency  $n$ , and therefore

$$g_R = \sqrt{2 \times \ln(3600n)} + \frac{0.577}{\sqrt{2 \times \ln(3600n)}} \quad (20)$$

Solaria [23] proposed  $g_D$  as Eq. (21); it's nearly to (20)

$$g_D = \sqrt{1.175 + 2 \ln \cdot n \cdot T_0} \quad (21)$$

In the broadband region, Eq. (19) has been evaluated, giving  $g_B \cong 3.5$  [22]. Using these factors, the maximum total load effect may be obtained by summing the mean load effect together, the factored broad-band and narrow-band load effects as follows

$$E_{max} = \bar{E} + [(g_B \sigma_{BE})^2 + (g_D \sigma_{DE})^2]^{1/2} \quad (22)$$

where  $\bar{E}$  is the value of the mean load effect;  $\sigma_{BE}$  is the *R.M.S.* value of the non-resonant load effect;  $\sigma_{DE}$  is the *R.M.S.* value of the resonant load effect. Thus, the total displacement of along-wind force acts on structure can be divided into two parts. First, the average displacement caused by average wind speed. Second, the turbulent displacement subjected to fluctuate by the turbulence. Therefore, the maximum tip displacement of structure subjected to along-wind force, given by

$$\begin{aligned}X_{max}(H) &= \bar{x}(H) + [(g_B \sigma_B)^2 + (g_D \sigma_D)^2]^{1/2} \\ &= \bar{x}(H) + x_{max}(H)\end{aligned}\quad (23)$$

where  $\bar{x}(H)$  is the value of tip displacement subjected to the mean wind speed;  $\sigma_B$  is the *R.M.S.* value of the non-resonant load effect;  $\sigma_D$  is the *R.M.S.* value of the resonant load effect.

$x_{max}(H)$  turbulent displacement that subjected to turbulence. Generally, GEF method is based on normal spectral methods as shown in Fig. 5 and some hypotheses. First, the GEF method is assumed a linearity of structure and single degree freedom model. Second, the  $G$  value consists of static, background and resonance factors; are assumed to have the same vertical distribution. Third, the GEF method is not considered in time variance for wind speed. For instance, from Eq. (23) the maximum displacement is obtained by

$$X_{max}(z) = \bar{x}(z) + x_{max}(z) = \bar{x}(z) \left(1 + \frac{x_{max}(z)}{\bar{x}(z)}\right) \quad (24)$$

where  $x_{max}(z) = g \cdot \sigma_x(z)$ ;  $g$  is a peak factor, the value of which is usually about 3 to 4.  $\sigma_x(z) = \sqrt{B^2 + R^2}$  is the *R.M.S.* value of the fluctuating displacement;  $B^2 = \int_0^\infty S_D(f) df$ ;  $R^2 = \frac{\pi \cdot f_0}{4 \cdot \zeta} S_D(f_0) \cdot S_D(f_0) = \frac{1}{k^2} \cdot |H(f)|^2 \cdot S_f(f)$  is the general coordinate of variance of internal loads;  $k$  is the stiffness of

structure.  $|H(f)|^2 = \frac{1}{\left[1 - \left[\frac{f}{f_0}\right]^2\right]^2 + 4\zeta^2 \left[\frac{f}{f_0}\right]^2}\right]^{1/2}}$  is the me-

chanical admittance function.  $f_0$  and  $\zeta$  are the natural frequency and damping ratio of the structure, respectively.  $|H(f)|^2$  is equal to 1 or zero for most structures, when  $\zeta$  is less than 0.05;  $f \approx f_0$ ; then the mechanical admittance function  $|H(f)|_{\max} \cong \frac{1}{2\zeta}$ .

$S_F(f)$  is a spectrum of wind force.  $\bar{x}(z)$  is the maximum fluctuating displacement of mean wind velocity at the average of  $z$  height as follows

$$\bar{x}(z) = \sum_{i=1}^H \frac{\int_0^H \bar{p}(z) \cdot x_i(z) dz}{4\pi^2 \cdot f_i^2 \cdot M_i} x_i(z); M_i = \int_0^H x_i^2(z) \cdot m(z) dz \quad (25)$$

where  $\bar{p}(z)$  is refer to Eq. (7);  $f_i$  and  $m(z)$  are the natural frequency and mass per unit height of the structure, respectively. Therefore, ref. Eq. (23)~(25) the gust effect factor  $G(z)$  is defined as

$$G(z) = 1 + \frac{x_{\max}}{x(z)} \quad (26)$$

As for Eqs. (24) and (26), the maximum displacement  $X_{\max}(z) = G(z) \cdot \bar{x}(z)$  is able to account for the maximum fluctuating displacement of mean wind velocity multiplied by the gust effect factor  $G$  value at the average of  $z$  height. However, there are some simplifications methods for equivalent static wind loads. An attempt to consider dynamic effects on the response of these structures is made through the gust response factor (GRF) method suggested by Davenport [12]. A typical form of response for structures subjected to wind loading is illustrated in Fig. 6. The total response is formed by the three components: (i) Mean ( $\bar{r}$ ): mean response in time; (ii) Background ( $r_B$ ): the energy is spread over a broad range in the low frequency range; (iii) Resonant ( $r_{Rj}$ ): consists of a series of highly concentrated peaks centered on the natural frequencies of the structure. The total peak response  $r$  (rms value) is given by  $r = \bar{r} \pm g_R \cdot \sqrt{r_B^2 + \sum r_{Rj}^2}$  where the statistical peak factor  $g_R$  is given by Eq. (20). Furthermore, it is incorporated in the ASCE [5] guidelines for the loading of transmission towers, but with the resonant response component neglected. Therefore, the peak

response is changed by  $\hat{r} = \bar{r} \pm G \hat{r}_B \Rightarrow \bar{F}_d \cdot i_r \cdot G$  where  $\hat{r}$  is the design value of peak response of wind gust for HMS.  $\hat{r}_B = i_r \cdot \sqrt{\sum_{i=1}^n r_{PLi}^2}$  is the design value of response of background for HMS,  $i_r$  is an influence coefficient.  $r_{PLi}$  the response subjected to mean wind drag force applying to the shaft of  $i$ th section of HMS.  $\bar{F}_d$  the mean wind drag force, and the gust re-

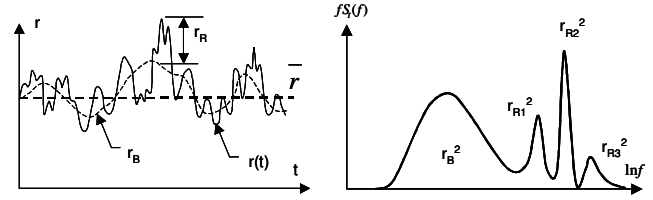


Fig. 6. Response of a structure to wind: (a) time history; and (b) power spectrum [7].

sponse factor  $G = 1 + 0.75 \cdot g_R \cdot E_X \cdot \sqrt{B_H + R_H}$  for the HMS,

the exposure factor  $E_X$  is given by  $E_X = \sqrt{24 \cdot k} \left(\frac{z_{ref}}{h_e}\right)^\alpha$  [18].  $z_{ref}$

is the reference height,  $h_e$  is the effective height (at approximate center of pressure of structure),  $\alpha$  is the power-law exponent,  $k$  is the surface drag coefficient [12]. The dimensionless response term corresponding to the quasi-static background wind loading

on the tower,  $B_H$  is given by:  $B_H = \frac{1}{1 + 0.375H/L_v}$ . ( $H$  the

tower's height and  $L_v$  the transverse integral scale of turbulence) The dimensionless resonant term  $R_H$  is given by:

$$R_H = 0.0123 \cdot \left(\frac{f \cdot h_e}{V_e}\right)^{-5/3} \cdot \frac{1}{\zeta} \quad [18] \text{ where } f \text{ is the tower's natural}$$

frequency,  $V_e$  is the mean wind speed at effective height  $h_e$  and  $\zeta$  is the tower's damping. The approach is based on statistical methods which considers the spatial correlation and energy spectrum of wind speed and the dynamic response of the HMS.

#### IV. WIND-EXCITED RESPONSE

There are several different phenomena with giving rise to wind-excited response for HMS. Three wind-excited phenomena were identified as possible sources of large-amplitude vibrations which could lead to failure, galloping, vortex shedding, and natural wind gusts. However, across-wind response is more likely to arise from vortex shedding or galloping, these motion-induced wind loads are significant for HMS. Consequently, these behaviors are also investigated in across-wind response for the WRD procedure. Furthermore, in order to obtain the critical wind velocity in across-wind force correctly. Therefore, Eigenvalue method is used to solve the natural frequency in higher modes of the tapered HMS.

##### 1. Lock-In

The wind load perpendicular to the wind direction may be in resonance with the structure, it's different from the resonance of machine. Lock-in effect is subjected to the vortex shedding frequency and structure natural frequency nearly; within certain range of wind velocities. Consequently, when the mean design wind speed  $V_h$  (m/sec) is greater than the critical wind speed  $V_{cr}(z)$ ; then the structure will fall in the resonance area. However, design wind speed should be followed the local code,

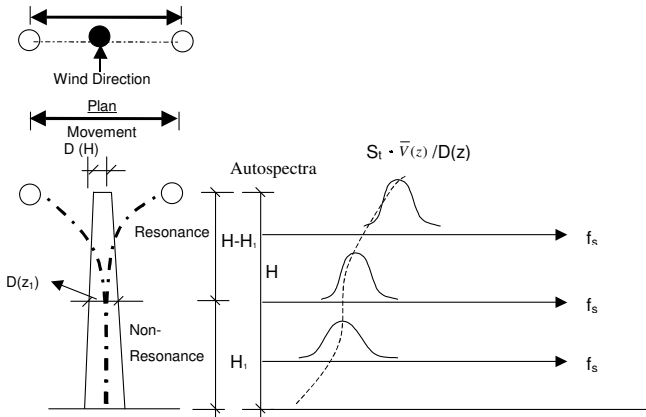


Fig. 7. Flow with turbulence decreasing diameter of HMS.

e.g. by the formula  $V_h = 40\sqrt{\mu_z(H)\mu_r\omega_0}$  as [9]. With the round cylinder as an example, when there is turbulence,  $S_t=0.2$ , and critical wind speed  $V_{cr}(z)$  value is obtained by Eq. (27)~(28)

$$S_t = \frac{f_s \cdot D}{V(z)} \quad (27)$$

$$V_{cr}(z) = \frac{5D}{T_j} \quad (28)$$

$f_s$  is the vortex shedding frequency;  $T_j$  is the natural period of structure ( $j=1, 2, \dots, n$ );  $D$  is the diameter of  $2/3H$  height. Across-wind loads due to vortex shedding in the first and second modes should be considered in the design of HMS when the critical wind speed  $V_{cr}$  is between 0.50 and 1.30  $V(z_{cr})$ ;  $V(z_{cr})$  is the mean design wind speed at  $z_{cr}$ ,  $z_{cr} = 5/6h$ , as [3].

Denoting the Strouhal number by  $S_t$ , the shaft-shedding frequency is  $f_s = \bar{V}(z) \cdot S_t / D$ ; since  $D$  is usually small,  $f_s$  is sufficiently high to justify the use of the quasi-steady theory [24]. On the other hand, the equivalent static pressure range to be used for fatigue design of vortex shedding-induced loads shall be followed as [2]

$$P_{vs} = \frac{0.613 \cdot V_{cr}^2 \cdot C_d \cdot I_F}{2 \cdot \beta} \quad (29)$$

where  $I_F$  is fatigue important factor;  $V_{cr}$  is expressed in m/s;  $C_d$  is drag coefficient and  $\beta$  is the damping ratio, which is conservatively estimated as 0.005, it is decreasing the damping of the structure with vortex shedding-induced in higher mode [2]. However, vortex shedding frequency  $f_s$  increases with the mean wind velocity  $\bar{V}(z)$  increases, and if the HMS width  $D$  is reduced. Therefore, the velocity profile of the wind, the turbulence of the wind field and a HMS width decreasing with height affects the across-wind net vortex shedding load on the HMS. Further, the net vortex shedding load occurs within a band of frequencies and not just at a specific frequency as shown in Fig. 7.

Special note that for HMS, when the critical wind speed exceeds the design wind speed, permitting modification of both

Table 2. The coefficient of drag derivatives [29].

Cross section	$R_e$	$\mu'_{DL}(0)$	Cross section	$R_e$	$\mu'_{DL}(0)$
→ 1 	66000	2.7	→ 1 	2000~20000	10.0
→ 1 	33000	3.0	→ 	75000	0.66

damping and the peak base moments, which significantly reduces the base moments [3].

## 2. Galloping

Galloping or Den Hartog instability is different from vortex shedding but also results in large-amplitude, resonant oscillation in a plane normal to the direction of wind flow as shown in Fig. 8. It is usually limited to structures with nonsymmetrical cross-sections, such as the plate-like as shown in Fig. 8(a) with attachments to the horizontal equipments or signal or cantilevered arm etc. as shown in Fig. 8(b). However, when the structure damping is equal to the aerodynamic damping, according to the differential equation of bending vibration of the cantilever structure, the critical wind velocity ( $v_{oc}$ ) is obtained by [28]

$$v_{oc} = \frac{2C_V}{\rho \cdot \mu'_{DL}(0) \cdot \int_0^H \sqrt{\mu_z(z)} \cdot B(z) \cdot \phi^2(z) dz} \quad (30)$$

where  $C_V = 2 \cdot M_V^* \cdot \xi_V \cdot \omega_V$  is generalized damping;  $M_V^* = \int_0^H m(z) \cdot \phi^2(z) dz$  and  $\omega_V$  are generalized mass and the natural circular frequency, respectively.  $\phi(z)$  is the shape function,  $\mu_z$  is the coefficient of wind pressure with height change. When  $\alpha=0$ ,  $\mu'_{DL}(0)$  is  $\mu_{DL}(\alpha)$  derived value,  $\alpha$  is a angle of wind with main x-direction, the equation is given by

$$\mu_{DL}(\alpha) = - \left[ \mu_D(\alpha) \cdot \frac{\sin \alpha}{\cos^2 \alpha} + \mu_L(\alpha) \cdot \frac{1}{\cos \alpha} \right] \quad (31)$$

where  $\mu_D(\alpha)$  is a coefficient of along-wind force or called the coefficient of drag force, it is equal to the absolute of summation for the front and back side. It is given by  $\mu_{DL}(\alpha) = \mu_{s1} + \mu_{s2}$ ;  $\mu_L(\alpha)$  is called the coefficient of across-wind force.  $\mu_D(\alpha)$  and  $\mu_L(\alpha)$  is obtained by wind tunnel test,  $\mu'_{DL}(0)$  is shown as in Table 2.

By conducting wind tunnel tests results, an equivalent static vertical shear of 1000Pa was determined for the galloping phenomena [1]. This vertical shear range should be applied to the entire frontal area of each of the sign or equipments attachments in a static analysis to determine stress ranges at critical connection details. The magnitude of this vertical shear pressure range shall be equal to the following:  $P_G = 1000 \cdot I_F$  (Pa) where  $I_F$  is fatigue important factor.

### 3. Comparison of Codes

GEF method is one of the simplified of equivalent static wind loads method. It has been adapted to along-wind loads on structure in most codes or standards, but does not include the requirements of the across-wind respond (e.g. deflection, vortex shedding, or instability due to galloping). The current engineering practice of WRD in Taiwan is based on the wind load provisions of the ASCE 7-02, with augment of across-wind wind loads from the AIJ-96 [4]. Tsai, Cherng, and Cheng revised ‘Establishment of building wind loading code and the associated commentary published in 1996’, their calculation formulas are based on ASCE 7-95 Code. Expecting that a correction factor of 1.443<sup>2</sup> is applied to accounting the difference between the wind speed averaging time adopted in Taiwan’s 2006 code (10 minutes) and that in ASCE 7-02 Code (3 seconds). ISO 4354 (International Standards Organization) proposed different wind speed at average time to convert with Eq. (32).

$$1.05V_{1hr} = V_{10min} = 0.84V_{1min} = 0.67V_{3sec} \quad (32)$$

The relationship between 3-sec. gust speed and any other averaging time can be found in texts by Simiu and Scanlon [21]. According to Taiwan 1996’s code, to calculate wind gust factor  $G(z)$  based on average roof high  $h$ , the height-width ratio is smaller than 5 or the natural periods is smaller than one second; then  $G(z)$  is according to

$$G(z) = 0.89 + 5.0 \cdot T(z) \quad (33)$$

$T(z)$  is intensity of turbulence given by

$$T(z) = \frac{2.35\sqrt{D_0}}{\left(\frac{z}{10}\right)^\alpha} \quad (34)$$

$D_0$  is the drag coefficient in different conditions of location. Wind gust factor  $G(z)$  given at period is greater than one second or the height-width ratio greater than by five of the structure by Eqs. (35) ~ (36).

(1) In respect to enclose building:

$$\bar{G} = 0.89 + \left[ 1.86 \cdot \frac{P}{\beta} + \frac{(4.52 \cdot T_1)^2 \cdot S}{1 + 0.00656 \cdot c} \right]^{1/2} \quad (35)$$

(2) In respect to open building:

$$\bar{G} = 0.89 + \left[ 2.32 \cdot \frac{P}{\beta} + \frac{(4.52 \cdot T_1)^2 \cdot S}{1 + 0.00328 \cdot c} \right]^{1/2} \quad (36)$$

$$P = J \cdot Y \cdot \bar{f} \quad (37)$$

$$\bar{f} = \frac{13.2 \cdot f_n \cdot h}{s \cdot V_{10}(C)} \quad (38)$$

where  $f_n$  is the natural frequency,  $\beta$  is damping ratio of the structure.  $T_1$  is the intensity of turbulence about 2/3 height of the structure from the ground.  $S$  is the size factor of structure;  $c$  is

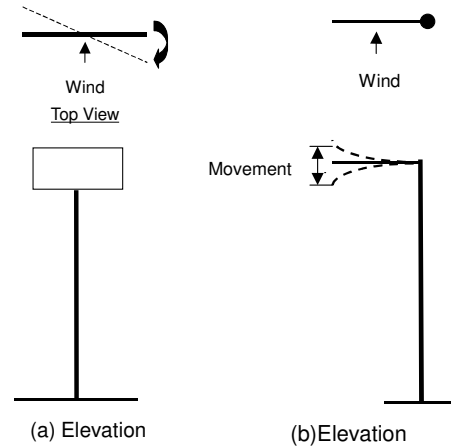


Fig. 8. Galloping subjected to bending moment or torsion.

the mean value with vertical of wind direction of the structure.  $J$  is the coefficient of pressure section.  $Y$  is the factor of resonance that is the function off  $\bar{f}$ .  $s$  is the factor of the roughness of ground surface [25]. The calculation of GEF procedure as Eqs. (33)~(38) has already been replaced by Closed Form Equation Method in Taiwan 2006’s code. For rigid structures, the minimum value of  $G(z)$  is adopted by 1.77 in Taiwan 2006’s code. The intensity of turbulence  $I_z$  and background response factor  $Q$  from Eqs. (39), (40) respectively; substitute into (41) to obtain the value of  $G(z)$ , these related coefficients as refer to [26].

$$I_z = c \cdot (10/\bar{z})^{1/6} \quad (39)$$

where  $c$  is listed in [26] for each exposure conditions;  $\bar{z}$  is the equivalent height of the structure defined as  $0.6h$  but not less than  $Z_{min}$  for all building heights  $h$ .

$$Q = \frac{1}{\sqrt{1 + 0.63 \left( \frac{B+h}{L_z} \right)^{0.63}}} \quad (40)$$

$B$  is a horizontal dimension of structure normal to wind direction;

$$G_f = 1.927 \left( \frac{1 + 1.7I_z \sqrt{g_Q^2 Q^2 + g_R^2 R^2}}{1 + 1.7g_V I_z} \right) \quad (41)$$

$R$  and  $L_z$  are resonant response factor and a integral length scale turbulence.  $g_Q$  and  $g_V$  should be used with 3.4,  $g_R$  should be given by Eq. (20).

Following is the wind pressure of the Support Structure Code of AASHTO (2001) as

$$P_{2001} = 0.613 \cdot K_z \cdot G \cdot V^2 \cdot I_r \cdot C_d \quad (N/m^2) \quad (42)$$

$P_{2001}$  is a wind pressure ( $N/M^2$ ),  $K_z$ , is a height and exposure factor.  $G$  is a wind gust effect factor (Min.=1.14);  $V$  is a peak

gust 3 sec in duration;  $C_d$  is a drag coefficient;  $I_r$  is an important factor. AASHTO 2001's code is updated from 1994's edition, the purpose is to change fastest mile of wind speed for 3 second. Therefore, AASHTO 2001's code adopted 1.14 ( $G=1.3 \times 0.82=1.07$ ) to meet the required minimum value of  $G$ .

China's latest code recommends the basic wind pressure ( $\omega_0$ ) in accordance with the Eq. (43).

$$\omega_0 = \frac{1}{2} \cdot \rho \cdot v_0^2 \tag{43}$$

Basic wind speeds  $V_0$  (m/s) is the maximum mean velocity at 10 minute with once every 50 years of recurrence at a height of 10 meter in spacious smooth ground and  $\rho$  is the air density. Substituting  $\omega_0$  into  $\omega_k$  as Eq. (44), one can find the along-wind pressure.

$$\omega_k = \beta_z \cdot \mu_s \cdot \mu_z \cdot \omega_0 \tag{44}$$

where  $\omega_k$  is load for wind standard value;  $\omega_0$  is the value of basic wind pressure.  $\beta_z$  is the wind gust coefficient at  $z$  height as shown in [9].  $\mu_s$  ( $=0.7 \sim 1.2$ ) is the body shape of wind coefficient for wind;  $\mu_z$  is the coefficient of the wind pressure with height change.

**V. WIND-RESISTANT DESIGN PROCEDURE**

Figure 9 indicates some interactions between different phenomena in the chain. The wind velocities were affected both by the wind climate or wind-induced (the first element as Fig. 9) and by turbulence in the atmospheric boundary layer (the second element as Fig. 9). It is important to control the critical velocity to avoid the vortex-shedding or galloping for the WRD (the third element as Fig. 9). Therefore, it should be check the critical wind speed condition caused by wind-excited in WRD procedure.

Analysis and propose in accordance with the regression of the power spectral formula of the typhoons wind speed of Taiwan. The suggestion from the range of natural frequency during 1~20 seconds should be followed the procedure of WRD [15]. Each link is necessary when wind-induced and the responses to behaviors are to be calculated or check. In wind engineering, all the mechanical responses (the forth element as Fig. 9) are caused by wind-induced, so the concept of a chain symbolized that the total design process is only as reliable as the links. This paper presents the steps relevant to the WRD criteria (as the first element to the fifth element as Fig. 9). The procedure for the wind-resistant design (WRD) of HMS can be broken into six steps. These steps, as outlined in the flowchart shown in Fig. 10(a)~(b); constitute the six major components of the general analysis procedure presented in this report. This general analysis procedure is briefly described as

**STEP 1: Construction of HMS model**

Construction of the finite element model of the HMS is

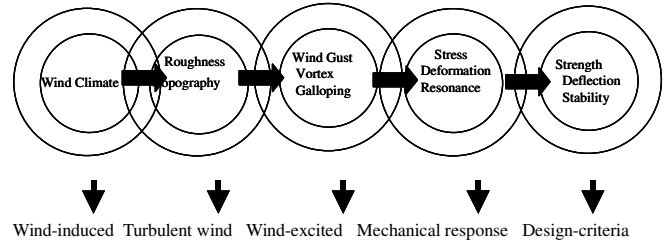


Fig. 9. Flow with turbulence decreasing diameter of HMS.

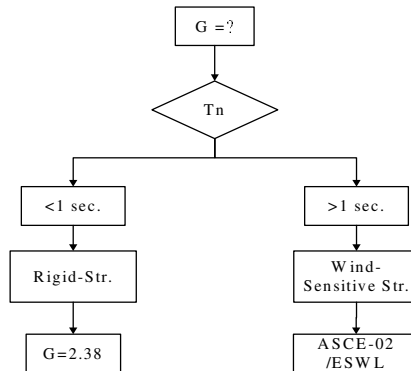
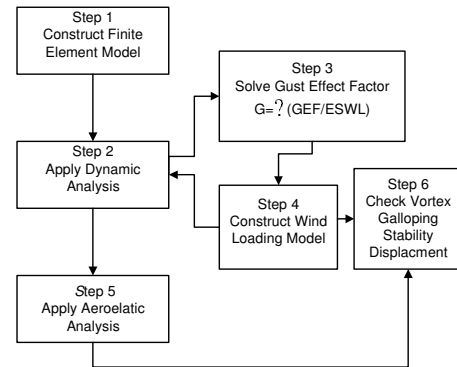


Fig. 10. (a) HMS of WRD procedure (b) calculation of GEF procedure.

shown in Fig. 1. Firstly, it should be determined the ratio of  $\frac{D}{t}$  to avoid the buckling of the shaft for wind loading is given by

$$\frac{D}{t} < 0.1259 \cdot \frac{E_s}{F_y} \tag{45}$$

$D$  is diameter of shaft,  $t$  is thickness of shaft,  $E_s$  is modulus of elasticity,  $F_y$  is yield stress. For round and multisided tubular members that have compact, non-compact, and slender element sections, the allowable bending stress could be computed according to AASHTO-2001 or ASD code. Secondly, the simulation adopt linear translational and rotational springs placed at the base of the HMS.

**STEP 2: Dynamic and aerodynamic analysis**

Eigenvalue analysis is performed in order to determine the rigidity or flexibility for the natural period of structure ( $T_n$ ) of the tapered of HMS. Furthermore, this paper suggests the Eq. (46) to check the effect of aerodynamic for HMS [19].

$$S_c = 4\pi \cdot K_s = \rho_s \cdot \frac{\xi}{\rho_a} > 5 \tag{46}$$

$K_s = m\xi/\rho d^2$ ;  $\xi$  is damping ratio of the structure (for steel structure  $\xi=0.02$ );  $\rho_a$  is air density ( $=0.125\text{kg}\cdot\text{s}^2/\text{m}^4$ );  $\rho_s$  is mass density of the structure. When Scruton number is less than 5, it's also determined to perform an aeroelastic analysis method (e.g. wind tunnel method) to obtain some parameters more accurately. Within the dynamic analysis, Steps 2 to 5 must also be performed in a repetitive fashion.

**STEP 3: Gust effect factor**

Typically, wind load in equivalent static wind loads as two methods. First, use mean wind pressure to add dynamic wind pressure. Second, multiply mean wind pressure by a dynamic factor. To obtain a dynamic factor, the value of  $G$  is adopted as shown in Fig. 10 (b). If designer want perform a more rigorous analysis to obtain the value of  $G$  as shown in Fig. 11.

**STEP 4: Construction wind loading model**

Construction of the wind-loading model to determine the loading applied to the finite element model (FEM). If the HMS is an importance of flexible structure, it's suggested to perform the aerodynamic analysis, or via wind time history method.

**STEP 5: Aeroelastic analysis**

The procedure of resolving the non-linear wind load forcing function is due to relative motion. The cause for this non-linearity is due to Morison's equation that is used to determine the force from the wind velocity in Eq. (47).

$$F = \frac{1}{2} \rho_{air} A C_d u_{wind} |u_{wind}| \tag{47}$$

where  $\rho_{air}$  is the mass density of air,  $A$  is the tributary projected area for the nodal point,  $C_d$  is the drag coefficient,  $u_{wind}$  is the wind velocity at the nodal point, and  $F$  is the force produced by the wind velocity. The true forcing function must be computed from the relative velocity between the pole and the wind.

**STEP 6: Procedure of check**

Across-wind loads due to vortex shedding should be considered in the design of HMS, when the critical wind speed  $V_{cr}$  is between 0.50 and 1.30  $V_h$  as defined here. Across-wind load is no need to consider, when it falls outside this range as shown in Fig. 12.  $V_h$  is the mean design wind speed (m/sec); in this study it can be obtained by local code ( e.g.  $V_h = 40\sqrt{\mu_z(H)\mu_r\omega_o}$  [9] ). Firstly, one can solve the Eq. (28) to determine the critical wind speeds for vortex shedding; the across-wind force is obtained by Eq. (48) [26].

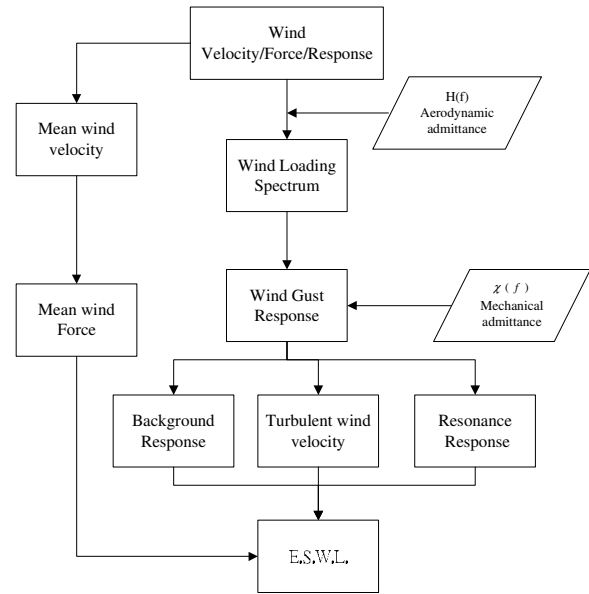


Fig. 11. Calculation of typical E.S.W.L. procedure.

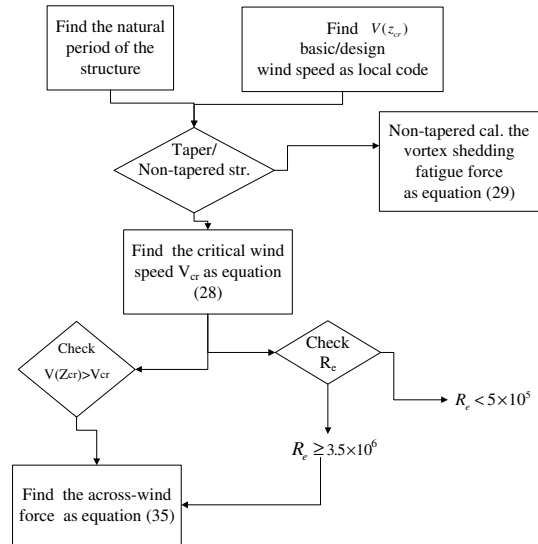


Fig. 12. Calculation of across-wind force procedure.

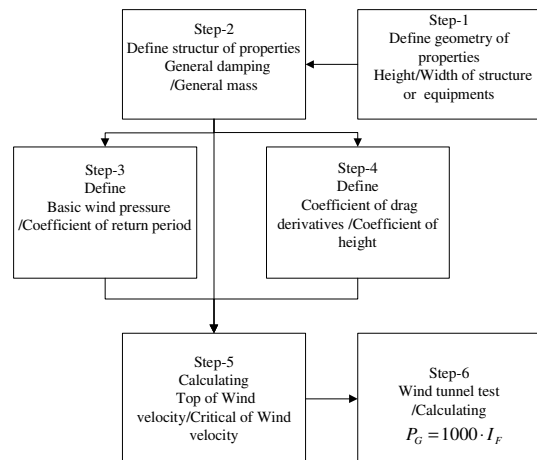


Fig. 13. Check galloping effecting procedure.

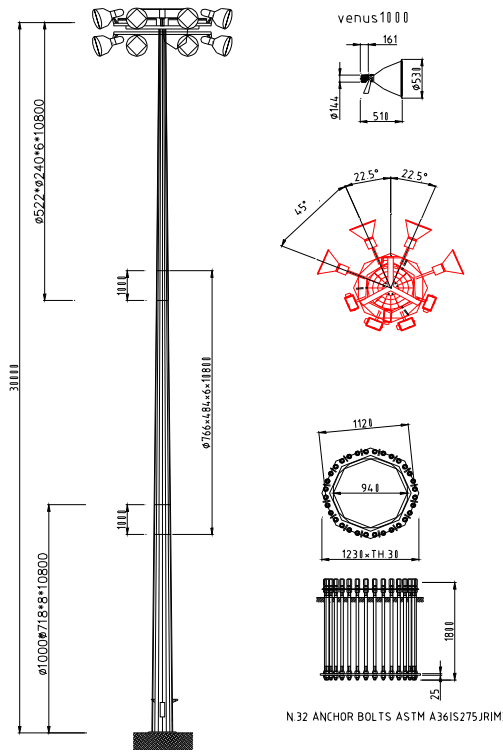


Fig. 14. High Mast Lighting Structure.

$$W_{rz} = U_r^2 \cdot \frac{Z}{h} \cdot C_r \cdot A \quad (48)$$

$W_{rz}$  is the across-wind force at height  $z$ ;  $U_r$  is the wind velocity of vortex resonance;  $C_r$  is the wind force of vortex resonance;  $A$  is project area of the structure. Furthermore, one obtained the tip displacement of HMS in across-wind force by accounting for Eq. (49) [28].

$$X_c = \frac{V_{cr}^2 \cdot D \cdot \phi(Z)}{8000 \cdot \xi \cdot m \cdot \omega^2} \quad (49)$$

$\xi$  is the damping ratio of structure;  $V_{cr}$  is critical wind speeds (m/sec);  $D$  is the diameter of structure.

Secondly, it can be obtained the value of galloping critical wind velocity ( $v_{oc}$ ) by the Eq. (30). It's needed to calculate the galloping force by wind tunnel test or formula:  $P_G = 1000 \cdot I_F$  as ref. [1, 2], when the value of galloping critical wind velocity  $v_{oc}$  is small than the mean design wind velocity or tip of wind velocity as shown in Fig. 13.

## VI. EXAMPLES

In order to quantify the implications of the above results with two structural examples are described below.

### Case-1 High mast lighting structure

For case-1, the taper of high mast lighting (HML) support structure, is adopt by Kaohsiung Mass Rapid Transport; one of applications from HMS. The shaft consists of three sections to

Table 3. Dimensional data of case-1 (mm)

Section n.	(1)	(2)	(3)	Total =(1)+(2) +(3)
Height	9400	9800	10800	30000
Laps length (upper joint)	1400	1000		
Laps length (lower joint)		1400	1000	
Total length	10800	10800	10800	
Thickness	8	6	6	
Base diameter	1000	766	522	
Diameter/Thickness	125	127	87	

Table 4. Case-1 Segments of wind gust factor (Taiwan-1996).

H(m)	$D_0$	$V_{10}$	$r$	J	S	Y	P	$\beta$	$T_1(2/3Z)$	$c/h$	G
(m/sec)											
30.00	0.25	95	0.0333	0.06	1.33	0.08	0.014	0.01	0.20	0.025	2.51
24.00	0.25	90	0.0417	0.06	1.33	0.08	0.012	0.01	0.21	0.031	2.38
19.90	0.25	86	0.0503	0.06	1.33	0.08	0.010	0.01	0.22	0.037	2.28
18.40	0.25	84	0.0543	0.06	1.33	0.08	0.010	0.01	0.22	0.040	2.24
11.40	0.25	74	0.0877	0.06	1.33	0.08	0.007	0.01	0.25	0.065	2.02
9.95	0.25	72	0.1005	0.06	1.33	0.08	0.006	0.01	0.26	0.074	1.96

Table 5. Case-1 segments of wind gust factor (Taiwan-2006).

NODE	h	B	L	$I_z$	$V_{10}$	$N_1$	Q	$R_n$	R	$R_B$	$R_L$	R	$G_f$
1	30.0	0.49	0.49	0.27	72.0	0.23	0.89	0.23	0.42	0.96	0.94	2.10	3.91
2	24.0	0.49	0.49	0.27	46.67	0.35	0.89	0.21	0.30	0.94	0.91	1.68	3.35
3	19.9	0.73	0.73	0.27	44.5	0.37	0.89	0.20	0.29	0.94	0.86	1.62	3.27
4	18.4	0.73	0.73	0.27	43.7	0.37	0.89	0.20	0.29	0.94	0.86	1.60	3.24
5	11.4	0.73	0.73	0.27	38.7	0.42	0.89	0.19	0.26	0.93	0.85	1.48	3.09
6	9.95	1.00	1.00	0.27	37.45	0.43	0.89	0.19	0.26	0.93	0.79	1.43	3.03

Table 6. Case-1 along-wind force of codes calculation (V=72m/sec).

H(m)	Taiwan-1996 (KG)	AASHTO-2 001 (KG)	China-200 2 (KG)	Taiwan-200 6 (KG)
30.00	1999	1836	3558	2147
24.00	1668	1674	2179	1704
19.90	584	613	1061	608
18.40	2679	2859	1497	2820
11.40	689	816	986	770
9.95	4593	5597	2218	5192
Total	12212	13394	11499	13241

be assembled by the slip on joint as shown in Fig. 14.

The HML structure is a continuous taper with 16-polygons cross section monotubular structure manufactured from pressed steel sheet welded longitudinally.

Table 3 summarizes the main geometric properties, there is a set of luminaries (weight=1000kg) and E.P.A. (effect project area) is about 2 m<sup>2</sup> at the summit. To meet the requirements for

the client, the design wind velocity is adopted 72 m/s,  $\rho_s$  is equal to 204 ( $\rho_s = 4479/9 \cdot 8/2.24 = 204$ ).

First step, to check the aerodynamic factor,  $S_c$  is obtained to 32.65 ( $S_c = \rho_s \cdot \xi/\rho_a = 0.02 \times 204/0.125 = 32.65$ ); then the value of  $S_c$  is greater five. Therefore, aerodynamic analysis can be neglected in this example.

Second step, the calculation of G is based on Taiwan 1996's and 2006's code as shown in Table 4~5, the first mode shape of the structure is shown in Fig. 15(a). Further, along-wind force is 13241kg by Taiwan 2006's code, and it closed to the 13394kg of the AASHTO 2001's code as shown in Table 6.

Third step, the galloping of critical wind speed is check by Eq. (30)~(31) as shown in Table 7. It's large more than the design wind speed. Therefore, Case-1 is not susceptible to galloping-induced vibration.

Fourth step, as for checking the vortex shedding resonance Eq. (28) is used to compare the critical wind speed  $v_{cr}$  with the design wind speed  $v_h$  as shown in Table 8. However, when  $v_{cr} < 1.3v_h$  one should consider the across-wind force; it is nearly about 40% of along-wind force by Taiwan 2006's code as shown in Table 9.

Fifth step, The displacement of the Case-1 is 88.2 and 140 cm for along-wind loading (W.L.) and group loading (for dead loading (D.L.) plus W.L.), respectively.

**Case-2 Tower structure**

This case introduced the wind-power tower where is located in the Mi-lia [7, 8, 27]. Design of tower is made by steel structure with the piling foundation. In this study, assumed the shaft is a uniform type and the diameter is equal to 3m. The thickness of shaft is 15mm; the height is about 50m; the thickness of foundation is 80 cm as shown in Fig. 15(b).

First step, one can find wind pressure; basic wind pressure  $\omega_0$  is equal to 1.2 KN/m<sup>2</sup>;  $\mu_r$  is equal to 1 in return period of 50 years as [9].

Second step, the natural period was obtained by eigenvalue analysis; it's equal to 0.984 sec. as shown in Table 10 (control in first mode).

Third step, one should calculate the critical wind speed as Eq. (28) and the mean design wind speed  $V_h$  for checking the vortex shedding resonance is given by

$$v_{cr} = 5 \times 3 / 0.984 = 15.244 < V_h = 40 \sqrt{\mu_z(H) \mu_r \omega_0} = 40 \cdot \sqrt{2.03 \cdot 1.2} = 62.43 \text{ (m/sec)}. \text{ Consequently, one shall consider the across-wind force in the resonance area.}$$

Fourth step, the results of across-wind force shown in Table 11 is calculated by Eq. (48), the relative of coefficients as [26]. Along-wind displacement ( $X_a$ ) is calculated by Eqs. (23)~(25) as shown in Table 12.

Fifth step, in order to solve the tip displacement in across-wind respond is obtained by Eq. (49)

$$X_c = \frac{15.244^2 \times 3 \times 1 \times 50^4}{8000 \times 0.02 \times 3.515^2 EI} = \frac{2.204 \times 10^6}{EI} = 6.79 \text{ cm}$$

where  $\xi$  is the damping ratio of structure (=0.02);  $v_{cr}$  is equal to 15.244(m/sec). D is the diameter equal to 3 meters. Therefore,

**Table 7. Calculation galloping of Case-1.**

Description	Symbols	Data	Unit
Height	H	30	m
Width of lighting equipments	B	2.5	m
Category condition( $\alpha$ )	$\alpha$	0.32	
Coefficient of height	$\mu_z$	1.42	
Coefficient of return period	$\mu_r$	1.1	
Design wind pressure	W	3.24	KN/m <sup>2</sup>
Natural period	$T_j$	1.54	sec
Generalized mass	$M^*$	4.479	ton
Coefficient of drag derivatives	$\mu_{DL}^*$	3	
Generalized damping	$C_v$	0.3653	t/s
Tip of Velocity	$v(H)$	62.54	m/s
Critical of velocity	$v_{oc}$	65.37	m/s

**Table 8. Case-1& Case-2 across-wind resonance and fatigue force.**

n	$T_j$ (sec)		$V_{cr}$ (m/sec)		$V_h$ (m/sec)		across-wind resonance		across-wind fatigue force(kg)	
	case-1	case-2	case-1	case-2	case-1	case-2	case-1	case-2	case-1	case-2
1	1.541	0.984	2.47	15.24	72.00	62.40	$V_{cr} < 20\text{m/s}$	Lock-in	37	23868
2	1.541	0.984	2.47	15.24	72.00	62.40	$V_{cr} < 20\text{m/s}$	Lock-in	37	23868
3	0.246	0.223	15.45	67.26	72.00	62.40	Lock-in	$V_{cr} > 20\text{m/s}$	1462	23868
4	0.246	0.223	15.45	67.26	72.00	62.40	Lock-in	$V_{cr} > 20\text{m/s}$	1462	23868
5	0.073	0.2	52.05	75.00	72.00	62.40	$V_{cr} > 20\text{m/s}$	$V_{cr} > 20\text{m/s}$	16610	23868
6	0.073	0.2	52.05	75.00	72.00	62.40	$V_{cr} > 20\text{m/s}$	$V_{cr} > 20\text{m/s}$	16610	23868

**Table 9. Across-wind force of Case-1.**

Node	Z (m)	$D_m$ (m)	$U_r$	A (m <sup>2</sup> )	$U_r * D_m$	M (kg)	$\rho_f$	$\rho_f \sqrt{\beta}$	$C_r$	$W_c = U_r^2 \cdot \frac{Z}{h} \cdot C_r \cdot A$
										(across-wind force) (kg)
1	30.00	0.49	9.92	1.46	4.84	69.04	47.16	6.67	4.03	580.51
2	24.00	0.49	9.92	2.46	4.84	116.22	47.16	6.67	4.03	781.75
3	19.90	0.73	14.76	2.03	10.71	95.87	47.16	6.67	4.03	1183.39
4	18.40	0.73	14.76	3.09	10.71	145.51	47.16	6.67	4.03	1660.83
5	11.40	0.73	14.76	3.07	10.71	144.66	47.16	6.67	4.03	1022.94
6	9.95	1.00	20.33	0.73	20.33	34.19	47.16	6.67	4.03	400.38
$\Sigma$										5629.81

the maximum displacement ( $X_{max}$ ) was obtained as shown in Table 12.

The major observations and findings are summarized as follow

- (1) The vortex shedding is shown in Table 8; the critical wind velocity of Case-2 is higher than Case-1 in the first mode. It presents Case-1 of the critical wind speed for the first mode of vibration which is less than the 50% of the tip wind speed.

**Table 10. Case2-for non-taper tower of modal participating mass ratios.**

MODAL PARTICIPATING MASS RATIOS							
MODE	PERIOD	INDIVIDUAL MODE			CUMULATIVE SUM		
		(PERCENT)			(PERCENT)		
		UX	UY	UZ	UX	UY	UZ
1	0.983575	16.0200	49.2627	0.0000	16.0200	49.2627	0.0000
2	0.983575	49.2627	16.0200	0.0000	65.2826	65.2826	0.0000
3	0.223169	0.0000	0.0000	0.0000	65.2826	65.2826	0.0000
6	0.199591	0.0000	0.0000	0.0000	65.2826	65.2826	0.0000
7	0.159891	12.8564	7.5190	0.0000	78.1390	72.8016	0.0000
8	0.159891	7.5178	12.8562	0.0000	85.6569	85.6578	0.0000
9	0.128335	0.0000	0.0000	0.0000	85.6569	85.6578	0.0000
10	0.128265	0.0000	0.0000	0.0000	85.6569	85.6578	0.0000

**Table 11. Across-wind force of Case-2.**

Node	Z (m)	D <sub>m</sub> (m)	U <sub>r</sub>	A (m <sup>2</sup> )	U <sub>r</sub> *D <sub>m</sub>	M (kg)	ρ <sub>f</sub>	ρ <sub>f</sub> *√β	C <sub>r</sub>	(across-wind force) (kg)
1	50.00	3.00	15.24	15.00	45.73	707.40	47.16	6.67	4.03	14048.94
2	40.00	3.00	15.24	30.00	45.73	1414.80	47.16	6.67	4.03	22478.30
3	30.00	3.00	15.24	30.00	45.73	1414.80	47.16	6.67	4.03	16858.72
4	20.00	3.00	15.24	30.00	45.73	1414.80	47.16	6.67	4.03	11239.15
5	10.00	3.00	15.24	28.50	45.73	1344.06	47.16	6.67	4.03	5338.60
6	1.00	3.00	15.24	13.50	45.73	636.66	47.16	6.67	4.03	252.88
Σ										70216.58

**Table 12. Displacement of Case-2 (mm).**

Code	H	V <sub>h</sub>	X <sub>ave</sub>	X <sub>a</sub>	X <sub>c</sub>	X <sub>max</sub> = $\sqrt{X_a^2 + X_c^2}$
Unit	m	m/s	mm	mm	mm	mm
China	50	65.40	29.84	35.09	70.16	78.44
Taiwan	50	56.08	25.47	30.56	70.16	76.53

**Table 13. Susceptibility of types of the HMS to various wind-loading phenomena.**

Type of Structure	Galloping	Vortex Shedding	Natural Wind Gust
Chimney		●	●
Pole		●	●
H.MLighting	●	●	●
Monotubular Tower		●	●
Hyperbolic Cooling Tower		●	●
Wind-turbine Tower		●	●
Cantilevered Sign Structure	●		●
Luminaries Structure		●	●
Silo Structure			●

Note: ● indicates structure is susceptible to this type of loading

Therefore, it needs to check the vortex resonance area in higher modes. On the other hand, when the critical wind velocity is greater than 15~20m/s; the wind is generally too turbulent for

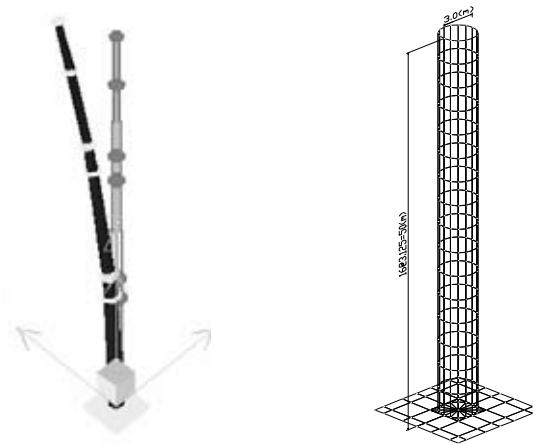


**Fig. 15. (a) Case-1 30m HMS, 1<sup>st</sup> mode=1.541(sec), top disp. =88.2cm. (b) Case-2 50m tower, 1<sup>st</sup> mode=0.984(sec), top disp. =4.2 cm.**

vortex shedding to occur.

(2) As is indicated in Table 13, not all of HMS mentioned is affected by all of these phenomena in WRD Procedure. For instance, in case-2, the blade of wind tower is free rotation, so it not leads to galloping effecting. To avoid and clarify these wind-induced vibration and instability behaviors subjected to along-wind or across-wind loading for line-like (e.g. Case-1) and point-like (e.g. Case-2) structure. It's should be adopted different method (e.g. check the tip displacement) and through the critical wind velocity to be controlled in the WRD procedure.

### VII. CONCLUSION

The results of the research reported herein indicate that

1. This study shows that the wind loads are key considerations in the HMS design; bodyweight does not severely affect the WRD in this investigation. According to the results of this research, the projected area is more critical in this aspect.
2. As for the intensity of wind excitation increases with increasing of aspect ratio (height-to-width). However, it decreases with increasing of structure damping. Consequently, the results of this research indicate that HMS is quite different from the tower structure. Furthermore, the body of the tip plays a major role in WRD. According to their shapes; it will either mitigate or exacerbate the oscillations.
3. This study shows that the natural periods of one second verification is better than the H/D (height to width) aspect ratio in the discrimination of rigidity or flexibility of HMS. It's recommended that an importance of HMS to be designed with natural period less than one second that a gust effect factor, G<sub>z</sub> of 2.38 be used for the design of rigid structure support for signs, signals, and luminaries. The value is greater than 1.77 for rigid structure according to the Taiwan building code 2006. Consequently, the designer should perform a more rigorous analysis when the G value is more than 2.38. As above the results of this research indicate that HMS is quite different from the traditional high-rise building.

## REFERENCES

1. AASHTO, *Supports Specifications*, the American Association of State Highway and Transportation Officials (1994).
2. AASHTO, *Supports Specifications*, the American Association of State Highway and Transportation Officials (2001).
3. ACI 307, *Design and Construction of Reinforced Concrete Chimneys*, American Concrete Institute (1998).
4. AIJ, *AIJ Recommendations for Loads on Buildings*, Architectural Institute of Japan (1996).
5. American Society of Civil Engineers, *Guidelines for Electrical Transmission Line Structural Loading*, ASCE Manuals and Reports on Engineering Practice No. 74, New York (1991).
6. ASCE 7-02, *Minimum Design Loads for Buildings and Other Structures*, American Society of Civil Engineers (2002).
7. Chien, C. W. and Jang, J. J., "Wind-resistant design of high mast structures," *Asia Pacific of Engineering Science and Technology*, Vol. 3, No. 2, pp. 549-570 (2005).
8. Chien, C. W. and Jang, J. J., "Dynamic analysis and design of tall tower structure," *Journal of Building and Construction Technology*, Vol. 2, No. 1, pp. 25-35 (2005).
9. China national standard (GB50009), *Load Code For The Design of Building Structures*, China Construction Industry Press (2001).
10. Cook, N. J., *The Designer's Guide to Wind Loading of Buildings. Part 2: Static Structures*, Butterworths: Building Research Establishment (1990).
11. Davenport, A. G., "The interaction of wind and structures," in: E. Plate (Ed), *Engineering Meteorology*, Elsevier Scientific Publishing Company, Amsterdam, pp. 557-572 (Chapter 12) (1982).
12. Davenport, A.G., "Gust response factors for transmission line loading," *Proceedings of the Fifth International Conference on Wind Engineering*, Colorado State University, Pergamon Press, Oxford (1979).
13. Dyrbye, C. and Hansen, S. O., *Wind Loads on Structures*, John Wiley and Sons Ltd, New York, (1997).
14. Hertig, J. A. "Some indirect scientific paternity of Alan G. Davenport," *Journal of the Wind Engineering and Industrial Aerodynamics*, No. 91, pp.1329-1347 (2003).
15. Jang, J. J., "Analysis of reliability of dynamic of the wind structure," *the Seventh Structure Engineering Seminars* (2004).
16. Johns, K. W. etc., "The development of fatigue design load ranges for cantilevered sign and signal support structures," *Journal of the Wind Engineering and Industrial Aerodynamics*, No. 77-78, pp. 315-326 (1998).
17. Lindt, J. W. van de and Goode, J. S., *Development of a Reliability-based Design Procedure for High-Mast Lighting Structural Supports in Colorado*, Colorado Department of Transportation Safety and Traffic Engineering Branch and Staff Bridge Branch (2006).
18. Loredou-Souza, A. M. and Davenport, A. G., "The influence of the design methodology in the response of transmission towers to wind loading," *Journal of Wind Engineering and Industrial Aerodynamics*, Vol. 91, pp. 995-1005 (2003).
19. Melbourne, W. H., "Predicting the across-wind response of masts and structure members," *Journal of the Wind Engineering and Industrial Aerodynamics*, No. 69-71, pp. 91-103 (1997).
20. Scruton, C., "On the wind excited oscillations of stack, towers and masts," in: *Proc. Wind Effects on Buildings and Structures*, HM Stationary Office, London, pp. 798-836 (1963).
21. Simiu, E., and Scanlan, R. H., *Wind Effects on Structures, 3rd Edition*, John Wiley and Sons, New York (1996).
22. Smith, J. W., *Vibration of Structures Application in Civil Engineering Design*, Chapman and Hall, New York (1988).
23. Solaria, G., "Alongwind response estimation: closed form solution," *ASCE Journal of the Structural Division*, Vol. 108, pp. 225-244 (1982).
24. Solaria, G., "Gust buffeting and aero elastic behavior of poles and monotubular tower," *Journal of the Fluids and Structures*, No. 13, pp. 877-905 (1999).
25. Tsai, I-C., Cherng, R.-H., and Hsiang, W. B., *Establishment of Building Wind loading Code and the associated Commentary*, Building research institute of Ministry of Internal Affairs (1996).
26. Tsai, I-C., Cherng, R.-H., and Hsiang, W. B., *Establishment of Building Wind loading Code and the associated Commentary*, Building research institute of Ministry of Internal Affairs (2006).
27. VESTAS Specification, *Wind System A/S Standard Foundation for Vestas V47-660/220 & V47-660/43.7M Tower*, VESTAS company (1998).
28. Wang, Z. M., *Tower Structure Design Manual*, China Construction Industry Press (1995).